ChemComm

ROYAL SOCIETY OF CHEMISTRY

COMMUNICATION

View Article Online
View Journal | View Issue

Cite this: *Chem. Commun.*, 2018, **54**, 13985

Received 19th October 2018,
Accepted 20th November 2018

DOI: 10.1039/c8cc08395a

rsc.li/chemcomm

OFF/ON switching of circularly polarized luminescence by oxophilic interaction of homochiral sulfoxide-containing *o*-OPEs with metal cations†

Pablo Reiné,[a] Ana M. Ortuño,[a] Sandra Resa,[a] Luis Álvarez de Cienfuegos,[a] Victor Blanco,[a] M. José Ruedas-Rama,[b] Giuseppe Mazzeo,[c] Sergio Abbate,[c] Andrea Lucotti,[d] Matteo Tommasini,[d] Santiago Guisán-Ceinos,[e] Maria Ribagorda,[e] Araceli G. Campaña,[a] Antonio Mota,[f] Giovanna Longhi,*[c] Delia Miguel*[b] and Juan M. Cuerva*[a]

Here we describe a new class of CPL switches based on oxophilic interactions between chiral sulfoxide-containing *ortho*-phenylene ethynylene (*o*-OPE) foldamers and cationic metals. These systems represent a unique case combining high g_{lum} values (up to 0.7×10^{-2}) and high quantum yields in both folded ON and unfolded OFF CPL states.

The search for new circularly polarized luminescence (CPL)-emitters based on small chiral organic compounds is of utmost relevance due to their promising optoelectronic applications.[1] CPL originates from the preferential emission of one handed circularly polarized radiation from an excited system[2,3] and it is usually characterized by the luminescence dissymmetry ratio $g_{\text{lum}} = 2(I_L - I_R)/(I_L + I_R)$, with I_L and I_R being the intensities of left and right circularly polarized emitted light. This preferential emission confers to the emitted light a new degree of freedom, which is a valuable parameter for further study and applications. Thus, for example, the modulation of the CPL emission of a chiral fluorophore using an external stimulus is interesting for smart sensing methodologies, to encode information in light or in patterning processes using security inks.[4–6] The possibility of switching ON the polarization without modifying the emission profile and/or the intensity of fluorescence is in fact especially challenging.

Within this context, we have recently described an easily accessible family of covalently locked and helically arranged *ortho*-phenylene ethynylenes (*o*-OPEs) as good CPL-emitters in terms of g_{lum} values (up to 1.1×10^{-2}).[7] Interestingly, similar helical arrangements were also obtained by a non-permanent process locking the folded conformation of sulfoxide-containing *o*-OPEs by carbophilic interactions with Ag(I) cations, opening the door to use these foldamers as chiroptical switches.[8] Nevertheless, the presence of Ag(I) cations directly bound to the fluorophore severely reduced the fluorescence quantum yield (QY) of the organic emitter.

To solve this drawback, in the present communication we have studied a new kind of OFF/ON CPL-switch[9] based on a new type of metal-promoted folding of *o*-OPEs able to give rise to novel foldamers having both high g_{lum} values (up to 0.7×10^{-2}) and significant QYs (38–84%) in both ON and OFF CPL-states. The emission profile is very similar for the coordinated and uncoordinated systems, resulting in one of the scarce examples of genuine creation of circular polarization in an existing emission process.[10] The switching mechanism relies on oxophilic metal cations which are able to promote the folding process by interacting with the oxygen atoms of both terminal sulfoxide groups (Fig. 1). We chose Ca(II), Sc(III), Mn(II), Co(II), Zn(II) or Ga(III) cations as representative examples (for all the studied metals see the ESI†).

Enantiopure sulfoxides containing *o*-OPEs (*S*,*S*)-**1**[8] and (*S*,*S*)-**2** (Fig. 1) were prepared using Sonogashira coupling reactions (see the ESI†). Their (chiro)-optical properties were then studied in the presence of different oxophilic metals with different oxidation states and magnetic behaviours.[11] Firstly, the coordination capabilities of (*S*,*S*)-**1** and (*S*,*S*)-**2** were studied by circular dichroism (CD), as presented in Fig. 2. This technique is interesting since the observed spectra presented evident changes upon metal complexation; besides that, CPL is related to the CD-active band at the longest wavelength and valuable information can be obtained from it. For such free ligands, CPL-active conformations,

---

[a] Department of Organic Chemistry, Faculty of Science, Universidad de Granada (UGR), E-18071 Granada, Spain. E-mail: jmcuerva@ugr.es
[b] Department of Physical Chemistry, Faculty of Pharmacy, UGR, Spain
[c] Department of Molecular and Translational Medicine, Università di Brescia, Brescia, Italy
[d] Department of Chemistry, Materials, and Chemical Engineering "G. Natta", Politecnico di Milano, Milano, Italy
[e] Department of Organic Chemistry, Faculty of Science, UAM, Spain
[f] Department of Inorganic Chemistry, Faculty of Science, (UGR), Spain

† Electronic supplementary information (ESI) available: Synthesis, structural characterisation, binding studies, computational methods, crystal and structure refinement data of the (*S*,*S*)-**2**:Zn(II) complex and additional figures and tables. CCDC 1871394. For ESI and crystallographic data in CIF or other electronic format see DOI: 10.1039/c8cc08395a

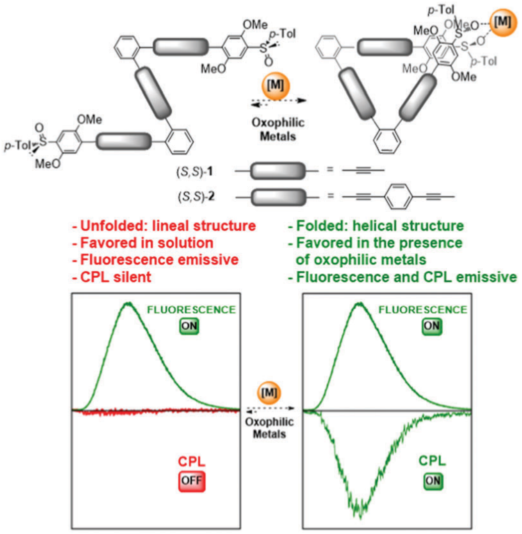

Fig. 1 Working hypothesis and structures of compounds (*S*,*S*)-**1** and (*S*,*S*)-**2**.

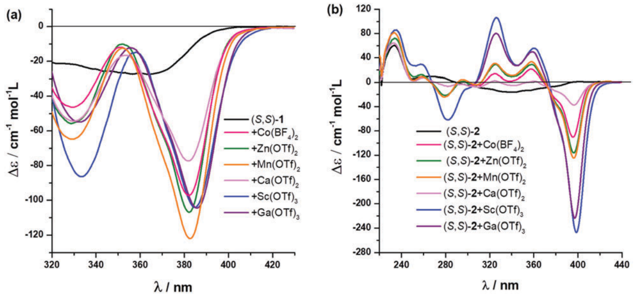

Fig. 2 CD spectra of (*S*,*S*)-**1** (a) and (*S*,*S*)-**2** (b) in the absence and presence of 30 equivalents of Ca(II), Sc(III), Mn(II), Co(II), Zn(II) or Ga(III) salts in a 9 : 1 mixture of CH_2Cl_2 : acetone as solvent.

the helically folded ones, are disfavoured in solution. In particular, the CD signal of free (*S*,*S*)-**2** at the longest wavelength ($\Delta\varepsilon = -16$ at 340 nm, $g_{abs} = -1.6 \times 10^{-4}$) was much lower than that previously recorded for (*S*,*S*)-**1** ($\Delta\varepsilon = -26$ at 360 nm, $g_{abs} = -6.8 \times 10^{-4}$) (black lines, Fig. 2), meaning that the OFF state is almost null and therefore a good OFF/ON switch could be expected. It is likely that the longer lateral arms in (*S*,*S*)-**2** significantly decrease the statistical population of folded conformations. Complexes of (*S*,*S*)-**1** with oxophylic tri- and divalent cations yielded very similar CD spectra, almost identical $\Delta\varepsilon$ values and very similar g_{abs} values at 390 nm ($\Delta\varepsilon = -(80\text{–}125)$, g_{abs}: Ca: -4×10^{-3}, Sc: -5.4×10^{-3}, Mn: -6.1×10^{-3}, Co: -5.5×10^{-3}, Zn: -7.5×10^{-3}, Ga: -5.4×10^{-3}), suggesting a similar arrangement of ligand (*S*,*S*)-**1** in all the complexes. Negative $\Delta\varepsilon$ values also indicated an induced *M*-helicity in the ligand after coordination, which differs from the *P*-helicity observed for carbophilic Ag(I) cation.[8] From the corresponding CD titrations we could extract the binding constants ($K_{Ca} = 9.5 \times 10^8 \pm 10\%\ M^{-2}$, $K_{Sc} = 6.4 \times 10^{10} \pm 18\%\ M^{-2}$, $K_{Mn} = 1.5 \times 10^{10} \pm 17\%\ M^{-2}$, $K_{Co} = 4.8 \times 10^{10} \pm 8\%\ M^{-2}$, $K_{Zn} = 1.2 \times 10^{10} \pm 11\%\ M^{-2}$, and $K_{Ga} = 1.0 \times 10^{10} \pm 8\%\ M^{-2}$) and a stoichiometry formula consistent with ((*S*,*S*)-**1**)$_2$:[M]. The same analysis was carried out for (*S*,*S*)-**2**, showing a similar behavior in CD spectra. Remarkably, in this case, after coordination, the g_{abs} values increased more than one order of magnitude from that of the free ligand ($\Delta\varepsilon = -(40\text{–}260)$, g_{abs} values: Ca: -3.6×10^{-3}, Sc: -8.3×10^{-3}, Mn: -5.7×10^{-3}, Co: -3.9×10^{-3}, Zn: -6.8×10^{-3}, Ga: -7.3×10^{-3}). The corresponding binding constants were also obtained ($K_{Ca} = 6.3 \times 10^6 \pm 55\%\ M^{-2}$, $K_{Sc} = 2.1 \times 10^9 \pm 21\%\ M^{-2}$, $K_{Mn} = 3.7 \times 10^9 \pm 17\%\ M^{-2}$, $K_{Co} = 6 \times 10^8 \pm 8\%\ M^{-2}$, $K_{Zn} = 1.8 \times 10^{10} \pm 84\%\ M^{-2}$, and $K_{Ga} = 1.6 \times 10^{10} \pm 21\%\ M^{-2}$), showing again a preference for the ((*S*,*S*)-**2**)$_2$:[M] stoichiometry.

A single crystal X-ray structure was obtained for the ((*S*,*S*)-**2**)$_2$:Zn(II) complex, confirming our initial structural assignment (Fig. 3a, see also the ESI† for the ((*S*,*S*)-**1**)$_2$:Ca(II) complex). The expected folded structure can be clearly observed, stabilized by a coordination mode using the oxygen atoms of the sulfoxide groups in an octahedral arrangement around the metal center completed by two solvent molecules. Accordingly, with the sign of the Cotton effect at the longest wavelength, the observed helicity of the OPE unit was *M*. Based on such X-ray structure, we theoretically modeled all other complexes in solution assuming the same octahedral coordination mode (Fig. 3b).[12]

The structures of the final diamagnetic complexes in solution were also studied by ^1H NMR spectroscopy, showing shielding of the signals corresponding to protons around the sulfoxide moiety, and thus suggesting a folded structure for the ligand. ^{13}C NMR showed that the chemical shifts of alkynes remained almost unchanged after coordination, in contrast to that previously observed by Ag(I) cations.[8]

Additional information could be obtained from vibrational CD (VCD) and Raman spectroscopy. VCD is quite sensitive to conformations (see Fig. 4 and the corresponding IR absorption spectra in Fig. S19, ESI†). The low VCD activity of (*S*,*S*)-**1** and (*S*,*S*)-**2** in CH_2Cl_2 solution is the result of their high flexibility.[8] Intensification of the signals in the presence of metal salts was indicative of a stabilizing effect of the metals on the phenylsulfoxide-OPE folded conformation. Considering Zn(II) complexes, different model geometries have been optimized starting from the X-ray structure (see Fig. S21 and S23 for calculated VCD and IR spectra with due comments, ESI†). The normal mode pattern in this spectroscopic region (phenyl C≡C-stretchings,

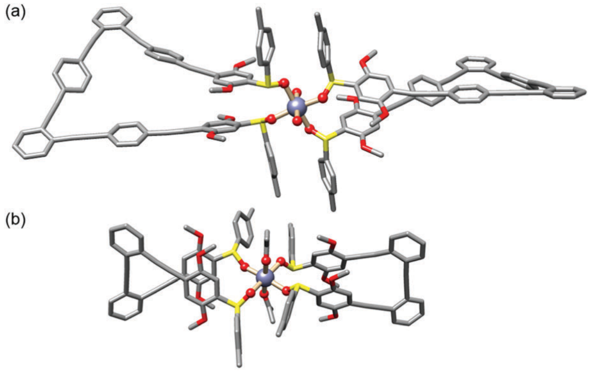

Fig. 3 (a) X-ray structure of the ((*S*,*S*)-**2**)$_2$:Zn(II) complex and (b) representative calculated structure for octahedral complexes of ((*S*,*S*)-**1**)$_2$:M(II). H atoms and counterions have been omitted for clarity.

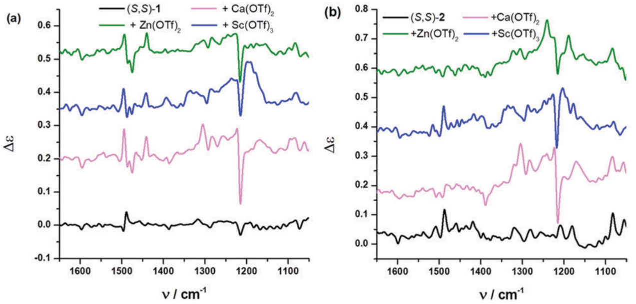

Fig. 4 VCD spectra in the mid-IR of the free ligands (black line) and those treated with about 5 equivalents of Ca(II) (pink line), Sc(III) (blue line), and Zn(II) (green line) salts for (a) (*S*,*S*)-**1** and (b) (*S*,*S*)-**2**. For the corresponding IR see the ESI.†

in plane bendings and methyl bendings) is highly conserved in the different models (see the ESI† for a better description). Some participation of the triflate counterion in generating VCD signals could not be excluded especially for (*S*,*S*)-**2**, as suggested also by the proposed calculated structures. The acceptable agreement between experimental and calculated VCD supported the conservation of the folded structures in solution, promoting a mutually oriented and strongly hindered phenylsulfoxide arrangement (Fig. 3), particularly in the case of (*S*,*S*)-**1** (Fig. S24, ESI†). Although the Raman technique does not distinguish in this case between folded and unfolded structures, interesting insight could be obtained, both in solution and in the solid state: oxophilic metals did not perturb the $C\equiv C$ bond in (*S*,*S*)-**1** (see Fig. S25 and S26, ESI†).[13] In the absence of coordination, $C\equiv C$ stretching modes were expected to lie nearby 2225 cm^{-1}.[14] DFT calculations (the same level as for VCD) were in good correspondence with Raman observations (see Fig. S27 and S28, ESI†). Similar data were also obtained for (*S*,*S*)-**2** upon coordination.[15]

Ligands (*S*,*S*)-**1** and (*S*,*S*)-**2** and metal complexes thereof were all fluorescent, although in both cases the QYs were higher in the absence of metals. For (*S*,*S*)-**1**, the QY varied between 8 and 39%, whereas in the case of (*S*,*S*)-**2** all the complexes retained high QY values, going from 86% without metal to a remarkable minimum of 34%. Regarding the polarized emission, (*S*,*S*)-**2** was almost CPL silent, in agreement with the very low g_{abs} value at the longest wavelength. On the other hand, (*S*,*S*)-**1** had previously shown a CPL response with a g_{lum} value of −0.001. Knowing the CPL response of the free ligands, we then measured their response in the presence of an excess of the corresponding Ca(II), Sc(III), Mn(II), Co(II), Zn(II), or Ga(III) cations (see the ESI† for the remaining metals). Despite their similarities in the CD spectra, the CPL responses were quite different instead. The diamagnetic metals showed an increase in the CPL signal with high g_{lum} values for (*S*,*S*)-**1** (Ca: -4.5×10^{-3}, Sc: -6.5×10^{-3}, Zn: -3.7×10^{-3}, and Ga: -3.3×10^{-3}) and (*S*,*S*)-**2** (Ca: -0.9×10^{-3}, Sc: -7.1×10^{-3}, Zn: -2.9×10^{-3} and Ga: -3.4×10^{-3}) in agreement with the corresponding g_{abs} values, thus evidencing closely related geometries of the ground and excited states.[16] Conversely, the CPL signals of complexes with paramagnetic metals, Mn(II) and Co(II), were much more weaker than and similar to those of the uncoordinated ligands

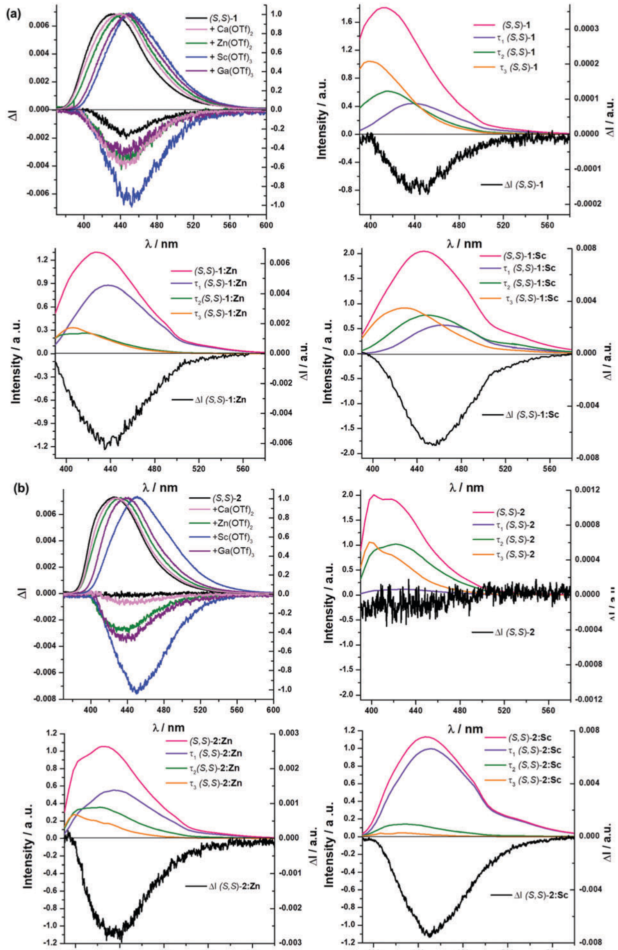

Fig. 5 Fluorescence and CPL spectra of (*S*,*S*)-**1** (a, top left) and (*S*,*S*)-**2** (b, top left) in the absence (black line) and presence of Ca(II) (pink line), Zn(II) (green line), Sc(III) (blue line), and Ga(III) (purple line) salts. The total fluorescence (pink line), SAEMS (τ_1 purple; τ_2 green; τ_3 orange lines) and CPL spectra (black line) of (*S*,*S*)-**1** (a) and (*S*,*S*)-**2** (b) in the absence (top right) and presence of Zn(II) (bottom left) and Sc(III) (bottom right) salts. See the ESI† for details.

(*S*,*S*)-**1** (g_{lum} Mn: -1.0×10^{-3}, Co: -1.1×10^{-3}) and (*S*,*S*)-**2** (Mn: -1.0×10^{-4}, Co: -1.1×10^{-4}).

To shed light on the origin of CPL emission, we obtained Time Resolved Emission Spectra (TRES) of (*S*,*S*)-**1** and (*S*,*S*)-**2** in the presence and absence of metals. Moreover, the areas of the species-associated emission spectra (SAEMS) gave us an idea of the proportion of the corresponding species. For all species, TRES analysis afforded three lifetimes around 4–7 (τ_1), 2–3 (τ_2) and 1 (τ_3) ns (see Fig. 5 and the ESI†).

These results indicated the presence of at least three emissive species in the excited state. Remarkably, in both free ligands (*S*,*S*)-**1** (Fig. 5a, top right) and (*S*,*S*)-**2** (Fig. 5b, top right) the circularly polarized emission (ΔI, black lines) is associated only with the species emitting at the longest wavelength ((τ_1), purple lines), as can be seen by comparison of the CPL signal with each of the emission spectra associated with each of the decay times (SAEMS: τ_1 purple; τ_2 green; τ_3 orange). This fact suggested that one of the free (*S*,*S*)-**1** emissive species was stable in the range of 5 ns (τ_1) and presented CPL-activity, being probably correlated with a folded structure in solution. The apparent g_{lum} value is modest due to the presence of species with non-polarized emissions (τ_2 and τ_3). In the case of (*S*,*S*)-**2** the contribution of the CPL-active excited state species is practically irrelevant. Taking into account the practically null CPL-response of free (*S*,*S*)-**2**, a build-up of CPL from zero could be observed in (*S*,*S*)-**2** upon metal coordination, especially in the case of Sc(III). For the complexes (*S*,*S*)-**1**:Zn (Fig. 5a, bottom left) and (*S*,*S*)-**2**:Sc (Fig. 5b, bottom right) we may again attribute the CPL emission (ΔI, black lines) to the species with the longest lifetime ((τ_1), purple line). The presence of non-polarized emissions from shorter lifetimes in the SAEMS spectra suggested that oligomeric material could also be present in solution. This seems to be the case for the (*S*,*S*)-**2**:Zn complex (Fig. 5b, bottom left). Additionally, in the case of the (*S*,*S*)-**1**:Sc complex (Fig. 5a, bottom right), the CPL emission could not be exclusively attributed to one species but to the combination of two close emissive species with the longest lifetimes (τ_1 purple and τ_2 green). All these studies suggested that the operating mechanism of the increased CPL activity of the diamagnetic complexes was the strengthening of the intrinsic contributions of the longest lifetime (τ_1) to the global emission by coordination with the ligand. For paramagnetic metals, the difference from the free ligand appears to be related to the presence of unpaired electrons, which affect particularly the CPL-active emission, as could be observed in the corresponding TRES and SAEMS analysis. The stability of the complexes was finally checked in different solvents. Remarkably, the complexes are formed and stable even in MeCN. Nevertheless, MeOH is able to reverse the equilibrium to the free ligand leading to an OFF/ON CPL switch.

In conclusion, we have shown that compounds (*S*,*S*)-**1** and especially (*S*,*S*)-**2** are able to fold by a novel oxophilic metal-mediated coordination mechanism, leading to stable complexes that present both high g_{lum} values and high QYs. A representative example is the (*S*,*S*)-**2**:Sc(III) complex, which has a g_{lum} value of -7.1×10^{-3} and keeps a good QY value of 0.38. Moreover, we have observed that the chiroptical properties of these complexes are influenced by the magnetic nature of the metal. These findings have been rationalized on the basis of the complete photophysical characterization of these systems. It is worth noting that these structures can finally act as CPL switches with high g_{lum} values while retaining the fluorescence profile in both ON and OFF states.

We thank the Ministerio de Economía y Competitividad (MINECO, Spain) (CTQ2017-85454-C2-1-P, CTQ2017-85454-C2-2-P, CTQ2015-70283-P) for funding. We also thank the UGR ''Unidad de Excelencia Química'' and PP2016-VS01 for support. A. G. C., P. R., S. R., and A. O. also acknowledge funding from MINECO and MECD (Spain) for RyC-2013-12943 and FPU contracts. Fondazione Cariplo and Regione Lombardia (Big & Open Data Innovation Laboratory, BODaI-Lab, University of Brescia), the Computing Center CINECA (Bologna), Italy, and CSIRC (UGR) are also acknowledged for access to computational facilities.

Conflicts of interest

There are no conflicts to declare.

Notes and references

1 B. A. San Jose, J. Yan and K. Akagi, *Angew. Chem., Int. Ed.*, 2014, **53**, 10641; F. Zinna, U. Giovanella and L. Di Bari, *Adv. Mater.*, 2015, **27**, 1719; R. Brandt, X. Wang, Y. Yang, A. J. Campbell and M. J. Fuchter, *J. Am. Chem. Soc.*, 2016, **138**, 9743; C. M. Cruz, I. R. Márquez, I. F. A. Mariz, V. Blanco, C. Sánchez-Sánchez, J. M. Sobrado, J. A. Martín-Gago, J. M. Cuerva, E. Maçôas and A. G. Campaña, *Chem. Sci.*, 2018, **9**, 3917; C. M. Cruz, S. Castro-Fernández, E. Maçôas, J. M. Cuerva and A. G. Campaña, *Angew. Chem., Int. Ed.*, 2018, **130**, 14998.

2 E. M. Sanchez-Carnerero, A. R. Agarrabeitia, F. Moreno, B. L. Maroto, G. Muller, M. J. Ortiz and S. de la Moya, *Chem. – Eur. J.*, 2015, **21**, 13488; J. Kumar, T. Nakashima and T. Kawai, *J. Phys. Chem. Lett.*, 2015, **6**, 3445; G. Longhi, E. Castiglioni, J. Koshoubu, G. Mazzeo and S. Abbate, *Chirality*, 2016, **28**, 696.

3 For recent examples see: J. F. Kögel, S. Kusaka, R. Sakamoto, T. Iwashima, M. Tsuchiya, R. Toyoda, R. Matsuoka, T. Tsukamoto, J. Yuasa, Y. Kitagawa, T. Kawai and H. Nishihara, *Angew. Chem., Int. Ed.*, 2016, **55**, 1377; S. Feuillastre, M. Pauton, L. Gao, A. Desmarchelier, A. J. Riives, D. Prim, D. Tondelier, B. Geffroy, G. Muller, G. Clavier and G. Pieters, *J. Am. Chem. Soc.*, 2016, **138**, 3990; N. Hellou, M. Srebro-Hooper, L. Favereau, F. Zinna, E. Caytan, L. Toupet, V. Dorcet, M. Jean, N. Vanthuyne, J. A. G. Williams, L. Di Bari, J. Autschbach and J. Crassous, *Angew. Chem., Int. Ed.*, 2017, **56**, 8236; T. R. Schulte, J. J. Holstein, L. Krause, R. Michel, D. Stalke, E. Sakuda, K. Umakoxhi, G. Longhi, S. Abbate and G. H. Clever, *J. Am. Chem. Soc.*, 2017, **139**, 6863; M. Gon, Y. Morisaki and Y. Chujo, *Chem. Commun.*, 2017, **53**, 8304.

4 Y. Imai, Y. Nakano, T. Kawai and J. Yuasa, *Angew. Chem., Int. Ed.*, 2018, **57**, 8973.

5 J. Andréassons and U. Pischel, *Chem. Soc. Rev.*, 2018, **47**, 2266.

6 J. Andres, R. D. Hersch, J. E. Moser and A. S. Chauvin, *Adv. Funct. Mater.*, 2014, **24**, 5029.

7 S. P. Morcillo, D. Miguel, L. Álvarez de Cienfuegos, J. Justicia, S. Abbate, E. Castiglioni, C. Bour, M. Ribagorda, D. J. Cárdenas, J. M. Paredes, L. Crovetto, D. Choquesillo-Lazarte, A. J. Mota, M. C. Carreño, G. Longhi and J. M. Cuerva, *Chem. Sci.*, 2016, **7**, 5663; P. Reiné, J. Justicia, S. P. Morcillo, S. Abbate, B. Vaz, M. Ribagorda, A. Orte, L. Álvarez de Cienfuegos, G. Longhi, A. G. Campaña, D. Miguel and J. M. Cuerva, *J. Org. Chem.*, 2018, **83**, 4455.

8 S. Resa, D. Miguel, S. Guisán-Ceinos, G. Mazzeo, D. Choquesillo-Lazarte, S. Abbate, L. Crovetto, D. J. Cárdenas, M. C. Carreño, M. Ribagorda, G. Longhi, A. J. Mota, L. Álvarez de Cienfuegos and J. M. Cuerva, *Chem. – Eur. J.*, 2018, **24**, 2653.

9 H. Maeda, Y. Bando, K. Shimomura, I. Yamada, M. Naito, K. Nobusawa, H. Tsumatori and T. Kawai, *J. Am. Chem. Soc.*, 2011, **133**, 9266; Y. Hashimoto, T. Nakashima, D. Shimizu and T. Kawai, *Chem. Commun.*, 2016, **52**, 5171; H. Isla, M. Srbo-Hooper, M. Jean, N. Vanthuyne, T. Roisnel, J. L. Lunkley, G. Muller, J. A. G. Willians, J. Autschbach and J. Crassous, *Chem. Commun.*, 2016, **35**, 5932; A. Homberg, E. Brun, F. Zinna, S. Pascal, M. Gorecki, L. Monnier, C. Besnard, G. Pescitelli, L. Di Bari and J. Lacour, *Chem. Sci.*, 2018, **9**, 7043.

10 K. Takaishi, M. Yasui and T. Ema, *J. Am. Chem. Soc.*, 2018, **140**, 5334.

11 To compare with previous data recorded with Ag(I) cations, a 9 : 1 mixture of CH_2Cl_2 : acetone was used as solvent.

12 The additional ligands in the crystal are two water molecules, which come from the crystallization conditions. In solution, acetone molecules may play the same role, and have been used as additional ligands during the theoretical calculations.

13 However, the carbophilic silver induces a large wavenumber shift in the $C\equiv C$ stretching Raman modes of (*S*,*S*)-**1**, and shows a strong interaction with $C\equiv C$ bonds (Fig. S28, ESI†).

14 M. Ceppatelli, L. Fontana and M. Citroni, *Phase Transform.*, 2007, **80**, 1085; D. C. Kennedy, C. S. McKay, L.-l. Tay, Y. Rouleaua and J. P. Pezacki, *Chem. Commun.*, 2011, **47**, 3156.

15 The $C\equiv C$ bonds of (*S*,*S*)-**2** are not influenced by Ag(I). Thus (*S*,*S*)-**1** presents a unique hosting cavity for Ag(I) formed by the cooperative interaction of the three alkynes (Fig. S29, ESI†).

16 H. Tanaka, Y. Inoue and T. Mori, *ChemPhotoChem*, 2018, **2**, 386.